# Power Loss Evaluation of a Surface Mounted Permanent Magnet Synchronous Machine During Two Hybrid Electric Vehicle Driving Cycles

**Phi Hung Nguyen [1], Emmanuel Hoang [2], and Mohamed Gabsi [3]**

[1] *SATIE Laboratory, ENS Cachan, pnguyen@satie.ens-cachan.fr*
[2] *SATIE Laboratory, ENS Cachan, hoang@satie.ens-cachan.fr*
[3] *SATIE Laboratory, ENS Cachan, gabsi@satie.ens-cachan.fr*

## Abstract
*The paper presents a surface mounted permanent magnet synchronous machine (SMPMSM) with distributed windings. The main focus of the paper is to provide a new calculation method of electric machine losses, including copper losses and iron losses at load. This method based on the separation of injected current in d-q axes and the developed iron loss models expressing the dependence between the flux density variations and these currents. This calculation is applied not only for an operating point of the machine but for thousands points represented by a driving cycle of a hybrid electric vehicle (HEV). The calculations are taken into account the flux-weakening and the non-linear magnetic material.*

## Keywords
*permanent magnet synchronous machines, loss evaluation, non-linearity, flux-weakening, hybrid electric vehicle*

## 1. INTRODUCTION
The HEV allows combining the advantages of the thermal and electrical motorization while minimizing their disadvantages [Chan et al., 2010; Zhu et al. 2008, Zhu et al., 2006]. That is why several researchers have studied novel technologies of electrical machines for this kind of application such as the asynchronous machine, synchronous machine, switched reluctance machine, switching-flux synchronous machine or axial flux machine [Chan et al., 2010; Zhu et al. 2008; Amara et al., 2009; De la Barière et al., 2008; Fakhfakh et al., 2008]. The HEV traction drives require an ability to operate at constant power over a wide speed range, good overload performance and high efficiency [Soong et al., 2002]. Due to the permanent magnet excitation, PM brushless machines are inherently efficient and hence have been extensively used for HEV applications [Zhu et al., 2008]. Then, surface mounted permanent magnet synchronous machines are popularly used in this application [Isfahani et al., 2008]. Also in this paper, we have proposed a SMPMSM with distributed windings (Figure 2).

For electrical machines, the iron losses computation is usually a very complex problem. Many authors [Zhu et al., 2002; Mi et al., 2003; Yamazaki et al., 2006; Seo et al., 2009; Tariq et al., 2009; Doffe et al., 2010; Chen et al., 2010; Barcaro et al., 2008; Ding et al., 2010] have proposed iron losses models to compute

the iron losses in the electric machines that the authors [Krings and Soulard, 2010] has made an overview and comparison of iron losses models for electric machines. However, all proposed iron losses models are to compute the iron losses at a desired speed/torque or some speed/torque values. We have not found in the literature an iron losses model applied for overall wide range of frequency yet. In [Yamazaki et al., 2006] [Seo et al., 2009; Doffe et al., 2010; Barcaro et al., 2008; Ding et al., 2010; Akhondi et al., 2009], the authors proposed the losses calculation for the hybrid electric propulsion specially, but, it's only for an operating point or some operating points of the vehicle. Unfortunately, the vehicle operates not only at one point or at some driving points but at various torque/speed points.

As a solution for the above-mentioned problem, this paper proposes a computation method of the average losses overall the driving cycle, including copper losses and iron losses. In this study, we have taken into account the flux-weakening.

All the computation and modeling in this paper are based on the bi-directional finite element analysis (FEA-2D) make with the software FEMM version 4.2.

## 2. APPLICATION AND STUDIED MACHINE
Two studied driving cycles are the Artemis-Urban and the Artemis-Road for the urban and road application, respectively (Figure 1). They have been received by industrial partners in the PREDIT (Programme de REcherche et D'Innovation dans les Transports terrestres) project supported by French National Agency of Research (ANR). They also are two driving cycles
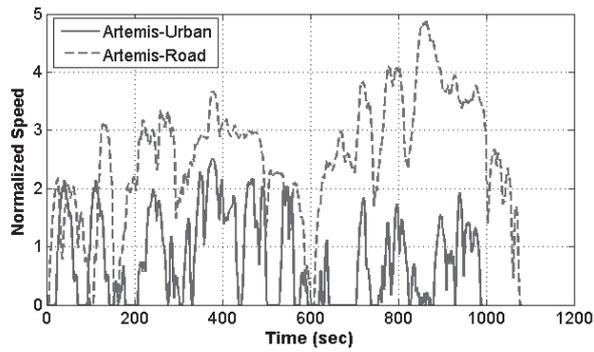
(a) Speed of the electrical machine
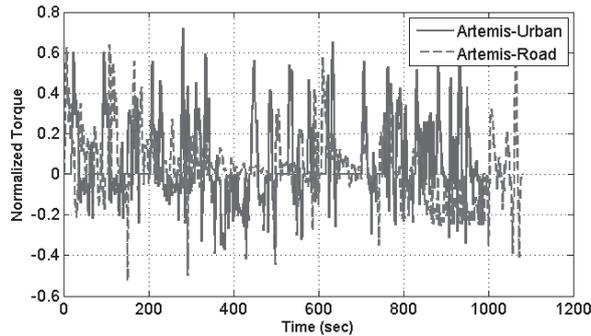


(b) Torque of the electrical machine
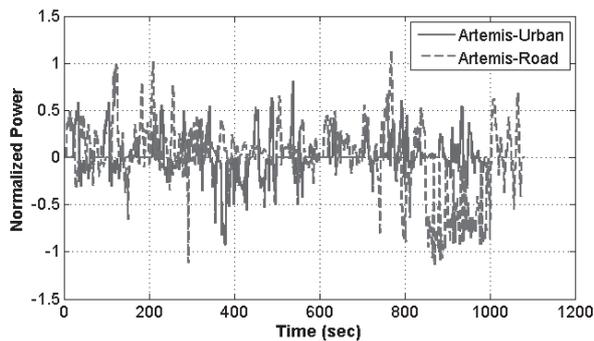


(c) Power of the electrical machine

**Fig. 1** Specifications of the electrical machine

**Table 1** Specification important parameters

| Parameter | Artemis-Urban | Artemis-Road |
|-----------|---------------|--------------|
| Max. torque, Nm | 150 | 134 |
| Max. speed, rpm | 4600 | 8870 |
| Average speed, rpm | 1400 | 4570 |
| Max. power, kW | 33 | 45 |
| Average power, kW | 4.8 | 10.5 |

there are some points that can attain a power around 40 kW but the values of the average power during the cycle are of 4.8 kW and 10.5 kW for Artemis-Urban and Artemis-Road, respectively.

As explained in the introduction, we have chosen a SMPMSM for this application. It is presented in Figure 2 is characterized by the distributed windings with 48 slots and 8 surface mounted permanent magnets ($B_r$ = 0.6T) on the rotor.
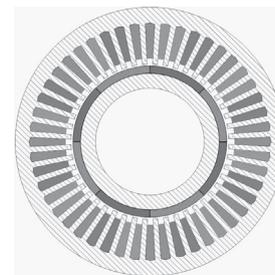


**Fig. 2** Studied electrical machine

**Table 2** Electrical machine parameters

| | |
|---|---|
| Pole number, 2p | 8 |
| Slot number, S | 48 |
| Radius of air-gap, mm | 58 |
| Air-gap width, mm | 0.6 |
| Stator external radius, mm | 100 |
| Stack length, mm | 200 |
| Tooth width, mm | 3.8 |
| Rotor inner radius, mm | 25 |
| Magnet height, mm | 5.0 |
| Slot fill factor, $k_s$ | 0.3 |

designed to imitate conditions encountered in a reproducible manner on European urban and road. They are mainly used for measuring vehicle consumption and emissions. The principle of these cycles is a "scenario" due to acceleration/deceleration and speed levels over a period of around 20 minutes. From the driving cycle analysis, we have defined a base point with a torque of 210 Nm and with a speed of 1820 rpm, so that the power at the base point is of 40 kW. If the machine operates at this point, it can operate at all torque points of the driving cycle.

Analyzing the driving cycle and basing on the base point, we have some important parameters such as the maximum torque, the maximum speed, the maximum power and the average power during the cycle, the number of points where the speed is higher than the base speed. Figure 1 and Table 1 have shown that

## 3. AVERAGE COPPER LOSSES DURING THE DRIVING CYCLE

### 3.1 Copper losses due to q-axis current

In this part, we have supposed that the magnetic circuit is unsaturated and that there aren't harmonics of current and of flux at no-load. Then, such as

this machine is a surface mounted permanent magnet machine, it does not show the saliency. Also with the above hypothesis, we have the well-known torque equation as the following [Nguyen et al., 2010]:

$$T_{em} = \frac{3}{2} . p . \Phi . I_q \qquad (1)$$

Where $p$ is the pole pair numbers, $\Phi$ is the maximum flux created by magnets, $I_q$ is the maximum stator $q$-axis current.

Consequently, from curves of the torque versus $q$-axis current density obtained by FEA, we have established the polynomial approximation of the average torque according to the q-axis RMS current density [Nguyen et al., 2010] (Figure 3):
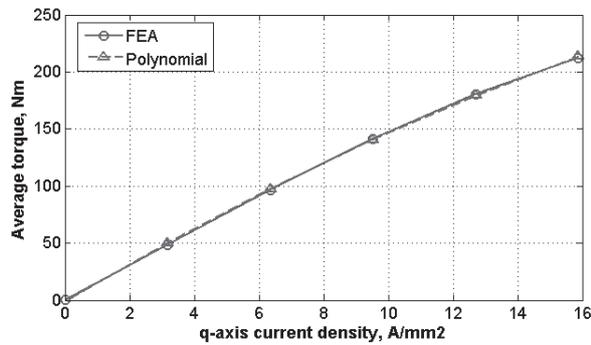


**Fig. 3** Torque versus q-axis current density

$$T_{em} = k_{t1} . \frac{\delta_q}{10} - k_{t2} . (\frac{\delta_q}{10})^2 \qquad (2)$$

Where $kt_1$, $kt_2$ are constants and $\delta_q$ is the $q$-axis RMS current density in A/mm$^2$.

### 3.2 Flux-weakening copper losses

In fact, when the machine works at the speed higher than the base speed, the machine needs the flux-weakening to acquire the desired speed. For this, it is necessary to inject the $d$-axis current with a negative
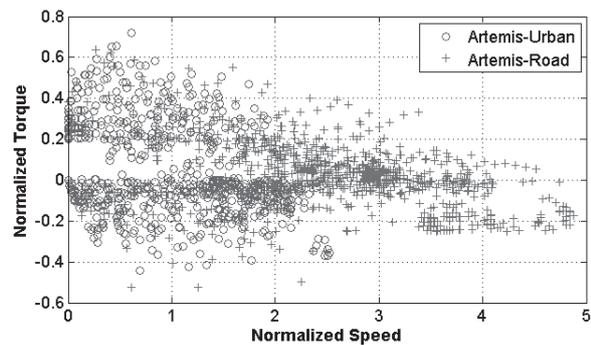


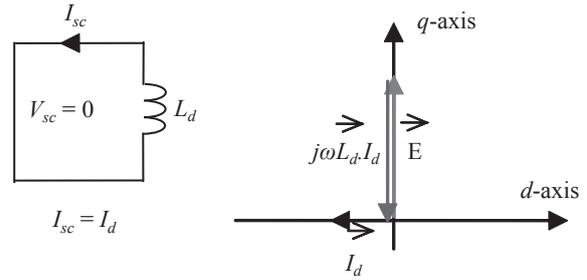**Fig. 4** Torque-speed specifications



**Fig. 5** Full flux-weakening in PMSM

value which decreases the flux created by PMs in the machine. To completely cancel the flux, the current is called short-circuit current $I_{sc}$. This principle has been shown on the Figure 5 [Soong et al., 2002; Ef-Refaie et al., 2005; Nguyen et al., 2010; Zhu et al., 2006].

According to Figure 4, the torque-speed characteristic of the driving cycle of the vehicle has shown that there are points where the speed is higher than the base speed (1820 rpm). Thus, the flux in the machine must be weakened at these points to obtain the desired speeds by the $d$-axis current injection.

Such as we have supposed that the torque don't depend on the $d$-axis current and that the machine has the infinite speed, from the Fresnel diagram analysis, we have a computation model of the flux-weakening current density as the following formula [Nguyen et al., 2010]:

$$\delta_{flux-weakening} = \delta_d = \delta_{sc} \left( 1 - \frac{N_b}{N} \right) \ if \ N > N_b \qquad (3)$$

Where $N$ is the speed at the studied point, $N_b$ is the speed at the base point, $\delta_{sc}$ is the short-circuit RMS current density.

Then, the copper losses model has been determined simply by the following formula:

$$P_{co} = \rho_{co} . L_a . (k_s . S_s . N_s) . (\delta_d^2 + \delta_q^2) \qquad (4)$$

Where $\rho_{co}$ is the copper resistivity, $L_a$ is the stack length, $k_s$ is the slot fill factor, $N_s$ is the lot number and $S_s$ is the slot section.

The objective of this calculation is to show the flux-weakening contribution on the losses during the driving cycle of the vehicle.

Figure 6 shows the distribution of copper losses du to $dq$-axe current for the two driving cycles.

Such as there are 38 % and 89 % point number that the speed is superior to the base speed, for Artemis-Urban and Artemis-Road, respectively, we have found that the machine has high average flux-weakening copper losses for the Artemis-Road while that of
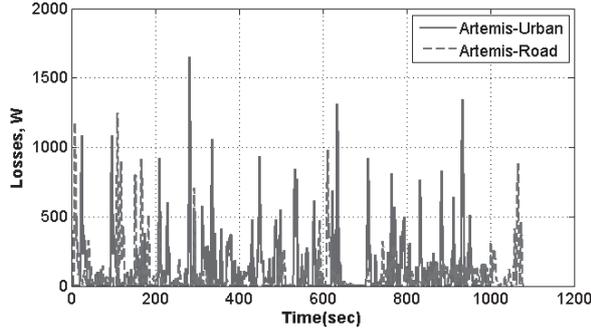
(a) Copper losses due to q-axis current distribution
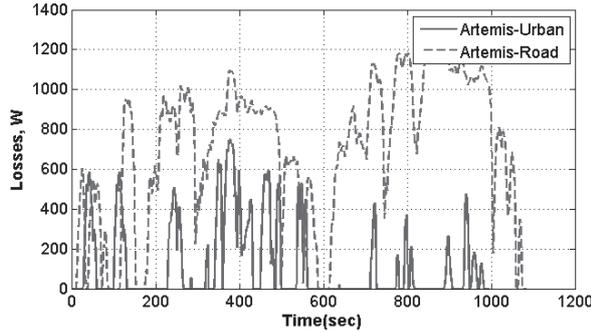


(b) Flux-weakening copper losses distribution

**Fig. 6** Copper losses distribution

**Table 3** Average copper losses during the cycle

| Copper losses due to | Artemis-Urban | Artemis-Road |
|---|---|---|
| $q$-axis, W | 104 | 65 |
| $d$-axis, W | 114 | 698 |

Artemis-Urban are lower. This result shows the difficulty of the SMPMSM for the flux-weakening at high speed.

## 4. AVERAGE IRON LOSSES DURING THE DRIVING CYCLE

In this paper, we propose a computation method of the iron losses at load during the driving cycle, including the flux-weakening. The computation of the iron losses is realized only on the stator.

Iron losses are divided in two parts: the first term, proportional to the frequency noted hysteresis losses, the second term, proportional to the square of the frequency is noted eddy current losses. Then, the iron losses model (W/m³) is:

- Iron losses by hysteresis:

$$P_{hys} = (k_{h1}.\Delta B + k_{h2}.\Delta B^2).f \qquad (5)$$

- Iron losses by eddy current:

$$P_{EC} = \alpha_p.\frac{1}{T}\int_0^T \left(\frac{db}{dt}\right)^2.dt = \alpha_p.\frac{1}{2\pi}\int_0^{2\pi}\left(\frac{db}{d\theta}\right)^2.d\theta.(2\pi f)^2 \qquad (6)$$

Where $f$ is the electric frequency; $\Delta B$ is the peak-to-peak value of flux density and $kh_1$, $kh_2$, $\alpha_p$ are constants which are determined from the constructor's data.

$$\alpha_p = \frac{d^2}{12\rho.\gamma} \qquad (7)$$

Where $d$ is the thickness of the electric sheet, $\rho$ is the specific resistivity and $\gamma$ the material density, $k_{h1} = 5$ (A.m⁻¹), $k_{h2} = 50$ (A.m.V⁻¹.s⁻¹) $\alpha_p = 0.042$ (A.m.V⁻¹).

Of course, the value of flux density is not the same in each part on the stator (Figure 7). The calculation of flux density value of each point on the stator could be a perfect idea but very difficult because of the computation time. Therefore, considering that there are some regions on the stator where flux density values are not too different, also, in order to have a better result, the stator of each machine has been divided into several small subdivisions in which the value of flux density is nearly constant.
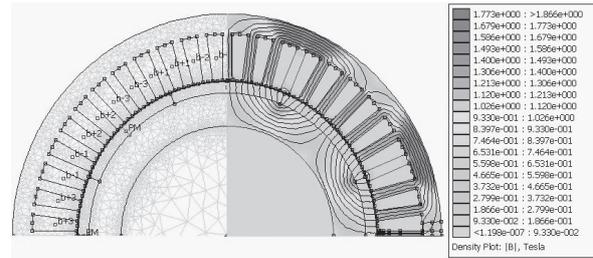


**Fig. 7** Flux density at no-load distribution



**Fig. 8** Subdivisions in a haft-stator tooth-yoke

We have developed "average value method". This method is based on the flux density analysis (FEA) of each subdivision on the stator and for the two axes Ox-Oy, and then, on the average analysis on the overall volume of the stator. Also from the formulas (5) and (6), we have developed the following formulas:

- Iron losses by hysteresis:

$$P_{hys} = (k_{h1}.\overline{\Delta B}_{h1} + k_{h2}.(\overline{\Delta B}_{h2})^2).f \qquad (8)$$

Where:

$$\overline{\Delta B}_{h1} = \frac{1}{V}.\sum_{i=1}^{n}\Delta B_i.V_i \qquad (9a)$$

$$\overline{\Delta B}_{h2} = \sqrt{\frac{1}{V}.\sum_{i=1}^{n} \Delta B_i^2 . V_i} \qquad (9b)$$

$N$ is the subdivision number of the stator; $\Delta B_i$ and $V_i$ are the peak-to-peak value of flux density during an electric period and the volume of the subdivision number $i$.

• Iron losses by eddy current:

$$P_{EC} = \alpha_p . \frac{1}{2\pi} \int_0^{2\pi} \left(\frac{db}{d\theta}\right)^2 . d\theta . (2\pi f)^2$$

$$= \alpha_p . \frac{1}{2\pi} . \sum_{k=1}^{m} \left[\frac{b_{k+1} - b_k}{\frac{2\pi}{m}}\right]^2 . \frac{2\pi}{m} . (2\pi f)^2 \qquad (10)$$

$$= \alpha_p . m . \sum_{k=1}^{m} (\Delta b_k)^2 . f^2$$

Where $m$ is the step number of the rotor rotation during an electric period $(2\pi_{elec})$.
Impose that for a subdivision $(i)$:

$$F_{ECi} = m . \sum_{k=1}^{m} (\Delta b_k)^2 \qquad (11)$$

We have deduced its average value overall the total volume:

$$\overline{F_{EC}} = \frac{1}{V} . \sum_{i=1}^{n} F_{ECi} . V_i \qquad (12)$$

And then, we have obtained:

$$P_{EC} = \alpha_p . \overline{F_{EC}} . f^2 \qquad (13)$$

In this section, we consider the influence of the flux-weakening and the injected current on the iron losses. From the presented models, we have obtained the following important parameters for each machine:
• $\delta_b = \delta_q$ is the $q$-axis current density creating the rated torque.
• $\delta_{sc} = \delta_d$ is the short-circuit current density for the flux-weakening in the machine.
The normalization of these values gives us:

$$\delta_q^* = \frac{\delta_q}{\delta_b} \quad \text{and} \quad \delta_d^* = \frac{\delta_d}{\delta_{sc}} \qquad (14)$$

Also from this normalization, we have made the discrimination of these values by five discrete steps between 0-1 and we have made the FEA for these values. With normalization and discrimination current values in both $d$-$q$ axes, we have calculated values of

$\overline{\Delta B}_{h1x}$, $\overline{\Delta B}_{h1y}$, $\overline{\Delta B}_{h2x}$, $\overline{\Delta B}_{h2y}$, $\overline{F}_{ECx}$ and $\overline{F}_{ECy}$. The objective of this calculation is to find the relationship of these average values versus $\delta_d^*$ and $\delta_q^*$. For this, we have formalized these relationships by the polynomial approximations as the following example for the $\overline{\Delta B}_{h1x}$. For $\overline{\Delta B}_{h1y}$, $\overline{\Delta B}_{h2x}$, $\overline{\Delta B}_{h2y}$, $\overline{F}_{ECx}$ and $\overline{F}_{ECy}$, the calculation is based on the same principle.

$$\overline{\Delta B}_{h1x} = F_0 + F_1 . \delta_d^* + F_2 . \delta_d^{*2} \qquad (15)$$

Where:

$$F_0 = f_{00} + f_{01} . \delta_q^* + f_{02} . \delta_q^{*2} \qquad (16a)$$

$$F_1 = f_{10} + f_{11} . \delta_q^* + f_{12} . \delta_q^{*2} \qquad (16b)$$

$$F_2 = f_{20} + f_{21} . \delta_q^* + f_{22} . \delta_q^{*2} \qquad (16c)$$

The values of $F_i$ $(i = 0, 1, 2)$ have been defined by the approximation of FEA calculations between the average values $(\overline{\Delta B}_{h1x}$, $\overline{\Delta B}_{h1y}$, $\overline{\Delta B}_{h2x}$, $\overline{\Delta B}_{h2y}$, $\overline{F}_{ECx}$ and $\overline{F}_{ECy})$ and the $d$-axis current for each $q$-axis current value. Then, the values of $f_{ij}$ $(i, j = 0, 1, 2)$ have been defined by the approximation of FEA calculations between the $F_i$ $(i = 0, 1, 2)$ and the $q$-axis current. The proposed calculation method of the average iron losses at load during the driving cycle respects the following order: An operating point $(i)$ on the cycle gives a torque value $T_i$ and a speed value $N_i$. For each
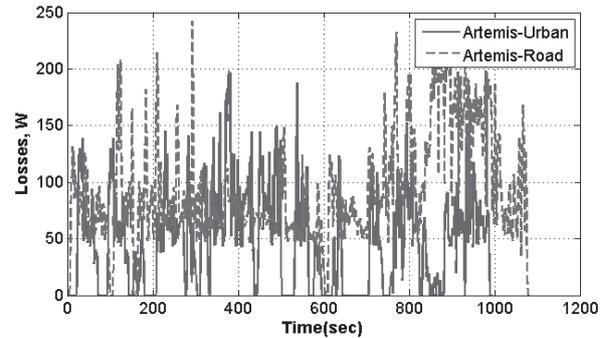


(a) Hysteresis iron losses distribution
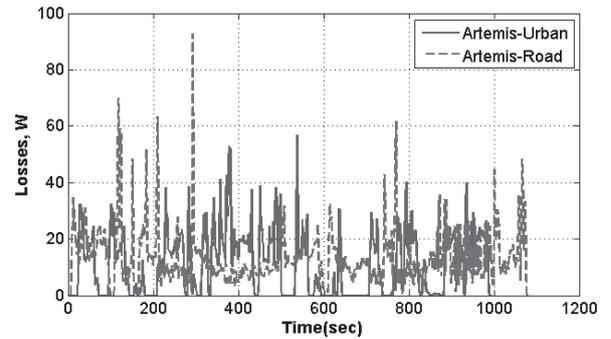


(b) Eddy current iron losses distribution

**Fig. 9** Iron losses distribution

point of the cycle, based on the models (2) and (3), we can determine the values of $\delta_{qi}$ and $\delta_{di}$, and then by formula (14), we have calculated values of $\delta_d^*$ and $\delta_{qi}^*$. Thus, knowing the value of $\delta_{qi}^*$, we can calculate the values of $F_{0i}$, $F_{1i}$ and $F_{2i}$ by formulas (16a), (16b) and (16c). Then, knowing the value of $\delta_{di}^*$, we can calculate the value of $\overline{\Delta B}_{h1x}$. This calculation has been applied similarly for $\overline{\Delta B}_{h1y}$, $\overline{\Delta B}_{h2x}$, $\overline{\Delta B}_{h2y}$, $\overline{F}_{ECx}$ and $\overline{F}_{ECy}$. Also, we can determine the iron losses value of this point (i) by formulas (8) and (13). And finally, the total value gives iron losses of this point. The same calculation has been done for other points of the cycle. Consequently, we could calculate the average value of iron losses at load during the driving cycle of the vehicle. Figure 9 shows the contribution of iron losses at load for the two driving cycles.

According to Figure 9, we have found that the iron losses at load are not high, specially the eddy current iron losses. This could be explained by the advantage of flux-weakening which reduces the flux density amplitude and the flux density harmonics in the core. Finally, the average efficiencies of the machine during the cycle are 94.6 % and 92.4 % for the Artemis-Urban and Artemis-Road, respectively (Table 4).

**Table 4** Average losses during the cycle

|  | Artemis-Urban | Artemis-Road |
|---|---|---|
| Hysteresis iron losses, W | 46 | 90 |
| Eddy current iron losses, W | 11 | 13 |
| Copper and iron losses, W | 275 | 866 |
| Efficiency, % | 94.6 | 92.4 |

## 5. CONCLUSION

In this paper, a surface mounted permanent magnet with distributed windings has been proposed and studied during two driving cycles of HEV. A computation method of average total losses of the machine during the driving cycle, including copper losses, flux-weakening copper losses and iron losses at load, has been presented. The advantages of this method are the possibility to be applied for any kind of permanent magnet machines without or with minor saliency and to take into account the non-linearity and the flux-weakening. Also, this calculation gives better precision with the specifications. However, the condition of the calculation is that all the traction forces are supplied by electric motor. The method also can apply only for series hybrid vehicle or battery electric vehicle.

## References

Akhondi, H., and J. Molimonfared, Design and optimization of tubular permanent magnet linear motor for electric power steering system, *Journal of Asian Electric Vehicles*, Vol. 7, No. 2, 1283-1289, 2009.

Amara, Y., L. Vido, M. Gabsi, E. Hoang, A. H. Ben Hamed, and M. Lécrivain, Hybrid excitation synchronous machines: Energy-efficient solution for vehicles propulsion, *IEEE Transactions on Vehicular Technology*, Vol. 58, No. 5, 2137-2149, 2009.

Barcaro, M., N. Bianchi, and S. Bolognani, Hybrid electric propulsion system using submersed SPM machine, *Proceedings of ICEM*, 2008.

Barière, O., H. B. Hamed, and M. Gabsi, Axial flux machine design for hybrid traction applications, *Proceeding of PEMD*, 2008.

Chan, C. C., A. Bouscayrol, and K. Chen, Electric, hybrid, and fuel-cell vehicles: Architectures and modeling, *IEEE Transactions on Vehicular Technology*, Vol. 59, No. 2, 589-598, 2010.

Chen, J. T., Z. Q. Zhu, S. Iwasaki, and R. Deodhar, Comparison of losses and efficiency in alternate flux-switching permanent magnet machines, *Proceedings of ICEM*, 2010.

Ding, X., M. Bhattacharya, and C. Mi, Simplified thermal model of PM motors in hybrid vehicle applications taking into account eddy current loss in magnets, *Journal of Asian Electric Vehicles*, Vol. 8, No. 1, 1337-1343, 2010.

Doffe, L., and M. Kadiri, Alternator contribution to $CO_2$ emission reduction policies, *Proceedings of ICEM 2010*, 2010.

EF-Refaie, A. M., and T. M. Jahns, Optimal flux weakening in surface PM machines using fractional-slot concentrated windings, *IEEE Transactions on Industry Applications*, Vol. 41, No. 3, 790-800, 2005.

Fakhfakf, M. A., M. H. Kasem, S. Tounsi, and R. Neji, Thermal analysis of a permanent magnet synchronous motor for electric vehicles, *Journal of Asian Eletric Vehicles*, Vol. 6, No. 2, 1145-1151, 2008.

Isfahani, A. H., and S. Sadeghi, Design of a permanent magnet synchronous machine for the hybrid electric vehicle, *International Journal of Electrical, Computer, and Systems Engineering*, Vol. 2, No. 1, 566-570, 2008.

Krings, A., and J. Soulard, Overview and comparison

of iron losses models for electric machines, *Proceeding of EVER*, 2010.

Mi, C., G. R. Slemon, and R. Bornert, Modeling of iron losses of permanent magnet synchronous motors, *IEEE Transactions on Industry Applications*, Vol. 39, No. 3, 734-742, 2003.

Nguyen, P. H., E. Hoang, M. Gabsi, and M. Lécrivain, A new method to find the fractional slot windings structures from a distributed slot windings permanent magnet synchronous machine and comparative study for a HEV application, *Proceedings of IEEE-ICIT 2010*, 2010.

Nguyen, P. H., E. Hoang, M. Gabsi, L. Kobylanski, and D. Comdamin, Permanent magnet synchronous machines: Performances during driving cycles for a hybrid electric vehicle application, *Proceedings of IEEE-ISIE*, 2010.

Seo, J. H., J. Y. Kwak, S. Y. Jung, C. G. Lee, T. K. Chung, and H. K. Jung, A research on iron loss of IPMSM with a fractional number of slot per pole, *IEEE Transactions on Magnetics*, Vol. 45, No. 3, 1824-1827, 2009.

Soong, W. L., and N. Ertugrul, Field-weakening performance of interior permanent-magnet motors, *IEEE Transactions on Industry Applications*, Vol. 38, No. 5, 1251-1258, 2002.

Tariq, A. R., C. E. Nino, and E. G. Strangas, A novel numerical method for the calculation of iron and magnet losses of IMPSMs, *Proceedings of IEMDC*, 2009.

Yamazakin, K., and Y. Seto, Iron loss analysis of interior permanent magnet synchronous motors-variation of main loss factors due to driving condition, *IEEE Transactions on Industry Applications*, Vol. 42, No. 4, 1045-1052, 2006.

Zhu, Z. Q., Y. S. Chen, and D. Howe, Iron loss in permanent magnet brushless AC machines under maximum torque per ampere and flux weakening control, *IEEE Transactions on Magnetics*, Vol. 38, No. 5, 3285-3287, 2002.

Zhu, Z. Q., and C. C. Chan, Electrical machines topologies and technologies on electric, hybrid, and fuel cell vehicles, *Proceedings of IEEE-VPPC*, 2008.

Zhu, Z. Q., Y. F. Shi, and D. Howe, Comparison of torque-speed characteristics of interior-magnet machine brushless AC and DC modes for EV/HEV applications, *Journal of Asian Electric Vehicles*, Vol. 4, No. 1, 843-850, 2006.